Research Article

Rapid Communications in Mass Spectrometry

Received: 29 June 2010 Revised: 15 September 2010 Accepted: 1 November 2010 Published online in Wiley Online Library: 00 Month 2010

Rapid Commun. Mass Spectrom. **2011**, *25*, 205–217
(wileyonlinelibrary.com) DOI: 10.1002/rcm.4846

Lyso-form fragment ions facilitate the determination of stereospecificity of diacyl glycerophospholipids

Weimin Hou[1,3], Hu Zhou[1,2], Maroun Bou Khalil[1,2], Deeptee Seebun[1,2], Steffany A. L. Bennett[1,2] and Daniel Figeys[1,2,3]*

[1]Ottawa Institute of Systems Biology, Faculty of Medicine, University of Ottawa, 451 Smyth Road, Ottawa, Ontario, Canada K1H 8M5
[2]Department of Biochemistry, Microbiology and Immunology, Faculty of Medicine, University of Ottawa, 451 Smyth Road, Ottawa, Ontario, Canada K1H 8M5
[3]Department of Chemistry, Faculty of Science, University of Ottawa, 10 Marie Curie, D'Iorio Hall, Ottawa, ON, Canada K1N 6N5

In this work we report the development of a novel methodology for the determination of stereospecificity of diacyl glycerophospholipids, including glycerophosphatidic acids (PA), glycerophosphoserines (PS), glycerophosphoglycerols (PG), glycerophosphoinositols (PI), and glycerophosphoethanolamines (PE), which can be conventionally ionized in negative ion mode. This methodology uses MS^2 recorded on a hybrid quadrupole time-of-flight mass spectrometer to determine the stereospecificity of diacyl glycerophospholipids based on the lyso-form fragment ions, attributed to the neutral loss of fatty acyl moieties. The fragmentation patterns of a variety of diacyl glycerophospholipid standards were first fully examined over a wide range of collision energy. We observed that lyso-form fragment ions corresponding to the neutral loss of fatty acyl moieties attached to the *sn2* position as free fatty acids ($[M–Sn2]^-$) and as ketenes ($[M–(Sn2\text{-}H_2O)]^-$) exhibited consistently higher intensity than their counterpart ions due to the neutral loss of fatty acyl moieties attached to the *sn1* position ($[M–Sn1]^-$ and $[M–(Sn1\text{-}H_2O)]^-$). Therefore, we concluded that an empirical fragmentation rule can be used to precisely determine the stereospecificity of diacyl glycerophospholipids, primarily on the basis of relative abundance of the lyso-form fragment ions. We then examined the product ion spectra of diacyl glycerophospholipids recorded from lipid extracts of rat hepatoma cells, where the stereospecific information of these lipids was conclusively determined. Combining the novel methodology reported in this work with the currently widely practiced mass spectrometric techniques such as multiple precursor ion scans (MPIS), fatty acyl scans (FAS), and multidimensional mass spectrometry based shotgun lipidomics (MDMS-SL), should enable a reliable and convenient platform for comprehensive glycerophospholipid profiling.

Mass spectrometry has become the method of choice for lipid identification and quantification.[1–7] Unlike protein analysis where the identification is a 'matching' process between the peptide fragments of a protein and its genomic prediction,[8] lipid identification is inherently a '*de novo*' process where the structural elucidation of a lipid species is based on the interpretation of mass spectrometry (MS)-derived structural information. In addition, due to the great structural diversity of lipid species,[9,10] there is no single platform capable of identifying all lipid species. Therefore, comprehensive lipid profiling of a biological system poses important technical challenges.

Glycerophospholipids play a wide variety of cellular roles in many eukaryotic cells and their fatty acyl compositions are important parameters in regard to the functions they play in a biological system. To date a diversity of mass spectrometric techniques have been successfully employed in elucidating structures of glycerophospholipids, where structural information pertaining to the polar head groups and fatty acyl moieties attached to the glycerol backbone can be obtained either in negative ion mode or positive ion mode with metal ion adduction.[11–20] In eukaryotic cells, the linkages of the fatty acyl moieties to *sn*2 positions are commonly always through esterification; while the bonding to s*n*1 positions could be acyl ester, alkyl ether, or vinyl ether linkages.[4] For diacyl glycerophospholipids, it is well documented that the relative abundance of the fragment ions pertaining to the two fatty acyl moieties is associated with their stereospecific position when they are subjected to fragmentation.[11–20] In negative ion low-energy tandem mass spectrometry mode, for diacyl glycerophosphatidic acids (PA) and diacyl glycerophosphoserines (PS) the fatty acyl anions lost from the *sn*1 position ($[FA1]^-$) always exhibit higher intensities than those lost from the *sn*2 position ($[FA2]^-$);[11,12] in contrast, for diacyl glycerophosphoglycerols (PG) and diacyl glycerophosphoethanolamines (PE), fatty acyl anions $[FA1]^-$ always exhibited lower intensities than $[FA2]^-$.[13,14] Therefore, attempts have been made to correlate the regiospecific positions of the two fatty acyl chains on the

* *Correspondence to:* D. Figeys, Ottawa Institute of Systems Biology, Faculty of Medicine, University of Ottawa, 451 Smyth Road, Ottawa, Ontario, Canada K1H 8M5.
E-mail: dfigeys@uottawa.ca

glycerol backbone for these diacyl glycerophospholipids versus the relative abundance of the two fatty acyl anions.[21–23] For diacyl glycerophosphoinositols (PI), however, the relative abundance of the two fatty acyl anions recorded in negative ion mode depends on the collision energy and the characteristics (e.g., length and number of double bonds) of the fatty acyl moieties.[15] Therefore, the stereospecific position number of the two fatty acyl chains cannot be determined using their relative abundance. Instead, it has been suggested that the stereospecificity of diacyl glycerophosphoinositols could be determined based on the relative abundance of their lyso-form fragments, which correspond to the neutral loss of free fatty acids ($[M–Sn1]^-/[M–Sn2]^-$) and the neutral loss of fatty acids as ketene ($[M–(Sn1\text{-}H_2O)]^-/[M–(Sn2\text{-}H_2O)]^-$), respectively.[15] Under low collision energy, it has also been observed for PA, PS, PG, and PE that the lyso-form fragment ions corresponding to the neutral loss of fatty acyl moieties from the *sn*2 position ($[M–Sn2]^-/[M–(Sn2\text{-}H_2O)]^-$) normally exhibit higher intensities than their counterparts ($[M–Sn1]^-/[M–(Sn1\text{-}H_2O)]^-$), which are associated with the neutral loss from *sn*1 position.[11–14] However, to date the structural information pertaining to the lyso-form fragment ions has not been fully exploited for the purpose of determining the stereospecificities of diacyl glycerophospholipids. One possible reason is that lyso-form fragment ions can only be recorded using either neutral loss scans or product ion scans. Unfortunately, monitoring large numbers of fragment ions for all the lipid species of interest using these approaches would require significant effort. However, large numbers of fatty acyl anions can be readily highlighted using multiple precursor ion scans (MPIS), fatty acyl scans (FAS), and multidimensional mass spectrometry based shotgun lipidomics (MDMS-SL).[7,24–27]

Shotgun lipidomic approaches usually analyze lipid extracts without or with very little pre-purification.[1,28,29] Most lipid species are thus analyzed under conditions subject to interferences from other isobaric species (or lipid species with molecular ion mass included within the isolation window for fragmentation) of the same class or other classes. As a result, the peak intensities of some fatty acyl anions of interest can be the sum of contributions from more than one lipid species. It is therefore very difficult to make correct positional assignments using MS techniques that look only at fatty acyl anions and neglect lyso-form fragment ions (e.g., FAS, MPIS, and MDMS-SL), especially when dealing with complex mixtures. In addition, lipid species that are not present in the mixture can also be wrongfully 'identified' (false-positives) by associating two fatty acyl anions that are actually from two different lipid species.

In order to exclusively identify glycerophospholipids, it is desirable to include the fragment ions that can provide connections between the fatty acyl moieties and their respective molecular ions. There are reports that the fatty acyl chain positions of diacyl phosphatidylcholines (PC) can be determined based on the relative abundance of their lyso-form fragment ions, which were recorded in MS^3 mass spectra on an ion trap mass spectrometer.[30]

In this work, we report a novel methodology to fully determine the stereospecificity of diacyl PA, PS, PG, PI, and PE. This methodology is based on the structural information derived from both the acyl anions and the lyso-form fragment ions from MS^2 obtained using a hybrid quadrupole time-of-flight (QqTOF) mass spectrometer. Unfortunately, previously published works[11–15] cannot provide all the information to develop this new methodology because factors such as type of mass spectrometer and collision energy can significantly affect fragmentation patterns.[23,31] Therefore, we examined a variety of diacyl glycerophospholipid standards, including PA, PS, PG, PI, and PE, over a wide range of collision energy. We found that the abundance of the lyso-form ions due to the neutral loss of free fatty acids and fatty acids as ketene from *sn*2 position remained consistently higher than the respective ions due to the neutral loss from *sn*1 position. The optimization of the collision energy for each lipid species allowed relatively abundant lyso-form fragment ions to be recorded in MS^2 spectra in negative ion mode. It is therefore feasible to assign the fatty acyl positions primarily based on the relative abundance of the lyso-form fragment ions for PA, PS, PG, PI, and PE. Using this methodology, we then analyzed fatty acyl compositions of glycerophospholipids in lipid extract from a rat hepatoma cell line overexpressing lipin-1α, a protein involved in lipid metabolism.[32,33] It was demonstrated that the present novel approach is capable of accurately determining the stereospecific information of diacyl glycerophospholipids even under interferences from other isobaric lipid species. In addition, the novel approach is capable of charting the fatty acyl moieties of diacyl glycerophosphoinositols, which is impossible for methodologies that monitor only fatty acyl anions.

EXPERIMENTAL

Materials and lipid standards

The diacyl glycerophospholipid standards used in this study were PA(12:0/13:0), PA(17:0/14:1), PA(17:0/20:4), PS(12:0/13:0), PS(17:0/14:1), PS(17:0/20:4), PG(12:0/13:0), PG(17:0/14:1), PG(17:0/20:4), PI(12:0/13:0), PI(17:0/14:1), PI(17:0/20:4), PE(12:0/13:0), PE(17:0/14:1), and PE(17:0/20:4). All the lipid standards were quantitative standards from Avanti Polar Lipids, Inc. (Alabaster, AL, USA). Chloroform and methanol were liquid chromatography grade from Fisher Scientific (Waltham, MA, USA). Ammonium acetate was purchased from Sigma Chemical Co. (St. Louis, MO, USA). Cell media and fetal bovine serum (FBS) were from Invitrogen (Carlsbad, CA, USA). Nanoelectrospray tips were purchased from New Objective (Woburn, MA, USA).

Cell culture and lipid extraction

The expression plasmid pcDNA3.1/V5-His-TOPO containing mouse lipin-1α coding sequences[34] was transfected into rat hepatoma McA-RH7777 cells using the calcium phosphate precipitation method, and stable transformants were obtained following selection with G418.[35] The cells were maintained at 37°C in a 5% CO_2 humidified incubator in Dulbecco's modified Eagle's medium (DMEM) supplemented with 10% FBS, 10% horse serum, 1% antibiotic-antimycotic solution (Invitrogen) and 200 μg/mL G418.

Lipids were extracted from rat hepatoma cells overexpressing lipin-1α ($\sim 4 \times 10^7$) with chloroform/methanol/acetic acid/saturated $NaCl/H_2O$ (4:2:0.1:1:2, v/v).[36] After

phase separation by centrifugation (1500 rpm, 15 min, 4°C), the organic phase fraction was collected and evaporated under a stream of nitrogen gas, followed by dissolving in 300 μL methanol.

Sample preparation and mass spectrometric analysis

A mixture of lipid standards was prepared by taking equal volumes of each lipid standard solution. The final concentration of each lipid standard was around 1 μM. After vortexing, the mixture of lipid standards was transferred to a QSTAR Pulsar QqTOF mass spectrometer (MDS Sciex, Concord, ON, Canada) using a syringe pump at a flow rate of 250 nL/min, controlled by Analyst software. For the lipid extract from rat hepatoma cells overexpressing lipin-1α, 50 μL of lipid samples were diluted with an equal volume of methanol, followed by spiking with 3 μL of ammonium acetate at a concentration of 250 mM so that the final concentration of ammonium acetate in the lipid sample was around 7.5 mM. The sample was then introduced into the mass spectrometer with the syringe pump at 250 nL/min.

The nanospray needle potential was set at −1200 V and the declustering potential (DP) was set at −30 eV. The mixture of lipid standards was first monitored by TOF MS until the total ion current (TIC) became stable. Product ion spectra of each lipid standard were then recorded sequentially at collision energies from 20 to 70 eV for PA, PS, PG, and PE, and from 20 to 80 eV for PI. Each product ion spectrum was recorded for 2 min to minimize the influence of signal intensity fluctuation. Quadrupole Q1 was operated at unit resolution.

For the analyses of the lipid extract from the lipin-1α cell line, precursor ion scans of *m/z* −153 and −196 were first performed to highlight molecular ions of PA/PS/PG/PI and PE, respectively. Quadrupole Q1 was operated at unit resolution and ~20 ms dwell time with step size of 0.3 Da. Product ion scans were then recorded for the lipid species of interest, each spectrum recorded for up to 2 min. For PI species, the collision energy was set at 55 eV. For all the other glycerophospholipids, the product ion scans were performed at 40 eV.

RESULTS AND DISCUSSION

Examining fragmentation patterns of diacyl glycerophospholipid standards under different collision energy

The fragmentation patterns of each individual glycerophospholipid class using negative ion mode have been studied previously.[11–15] However, because factors such as the type of mass spectrometer and collision energy can significantly affect fragmentation patterns,[23,31] previously published works cannot provide all the information required to develop the methodology reported in this work. Therefore, we first comprehensively analyzed tandem mass spectra of a range of diacyl glycerophospholipid standards in negative ion mode over a wide range of collision energy using a hybrid quadrupole time-of-flight mass spectrometer, in order to examine the feasibility of using the relative abundances of acyl anions and lyso-form ions to determine the stereospecificity of diacyl glycerophospholipids. Also the optimum collision energy, permitting the recording of measurable abundances of product ions suitable for structure elucidation, was determined for the different lipid standards.

This work was designed to examine all the diacyl glycerophospholipid species (PA, PS, PG, PI, and PE) that are conventionally analyzed in negative ion mode as a whole lipid class. The fragmentation patterns of PA standards are presented first, followed by comparisons of fragmentation patterns of PS, PG, PI, and PE standards with respect to that of PA. The similarities and differences in their fragmentation patterns can then be employed for comprehensive structural elucidation.

Fragmentation patterns of molecular anions diacyl PA as a function of collision energy

As described in the Experimental section, PA(17:0/14:1) was studied over a wide range of collision energy from 20 to 70 eV. Figure 1 shows representative tandem mass spectra of the molecular anion of PA(17:0/14:1), recorded at selected collision energies. The molecular ions were dominant in the spectrum recorded using a collision energy of 20 eV. Increasing the collision energy to 30 and 40 eV led to observation of abundant fragment ions corresponding to the two fatty acyl anions, polar head group, and 4 lyso-form fragment ions. Further increase of collision energy beyond 50 eV led to observation of only the two fatty acyl anions and the polar head group in high abundance.

Interestingly, the acyl anions $[FA1]^-$ were more abundant than $[FA2]^-$ over the range of collision (Fig. 2(a)) whereas the lyso-form fragment ions, corresponding to the neutral loss of free fatty acids and those resulting from neutral loss of fatty acids as ketenes $[M–Sn2]^-$ and $[M–(Sn2\text{-}H_2O)]^-$, were consistently higher than their counterpart ions $[M–Sn1]^-$ and $[M–(Sn1\text{-}H_2O)]^-$, respectively (Fig. 2(b)), in agreement with the previous study by Hsu *et al.* that used a triple-quadrupole mass spectrometer over a smaller collision energy range (25 to 35 eV).[11] When we ratio the signal intensities of these pairs of ions (Fig. 2(c)) we observe that the ratios of $[M–(Sn2\text{-}H_2O)]^-/[M–(Sn1\text{-}H_2O)]^-$ and $[M–Sn2]^-/[M–Sn1]^-$ were always higher than unity whereas the ratio of $[FA2]^-/[FA1]^-$ was always lower than unity. In this case, the length of fatty acyl chains attached to the *sn*1 position is longer than that bound to the *sn*2 position.

In order to ensure that the observed preferential loss of fatty acyl moieties at the *sn*2 position is not attributable to the lengths of the fatty acyl moieties, two other standards, PA(12:0/13:0) and PA(17:0/20:4), representing cases in which the length of fatty acyl chains attached to *sn*1 is close to and shorter than that bound to *sn*2, respectively, were studied following identical procedures. Identical conclusions can be drawn from these studies (Supplemental Fig. S1 of the Supporting Information shows that the signal intensities of $[M–Sn2]^-$ and $[M–(Sn2\text{-}H_2O)]^-$ were always higher than those of $[M–Sn1]^-$ and $[M–(Sn1\text{-}H_2O)]^-$, respectively). This result indicated that the preferred relative stereospecific abundances of lyso-form fragment ions and acyl anions of diacyl PA are independent of the lengths of their fatty acyl moieties. It follows that, in the absence of interferences from other lipid species, the relative abundance of both the acyl anions and the lyso-form fragment ions can facilitate the determination of the regiospecificity of diacyl PA.

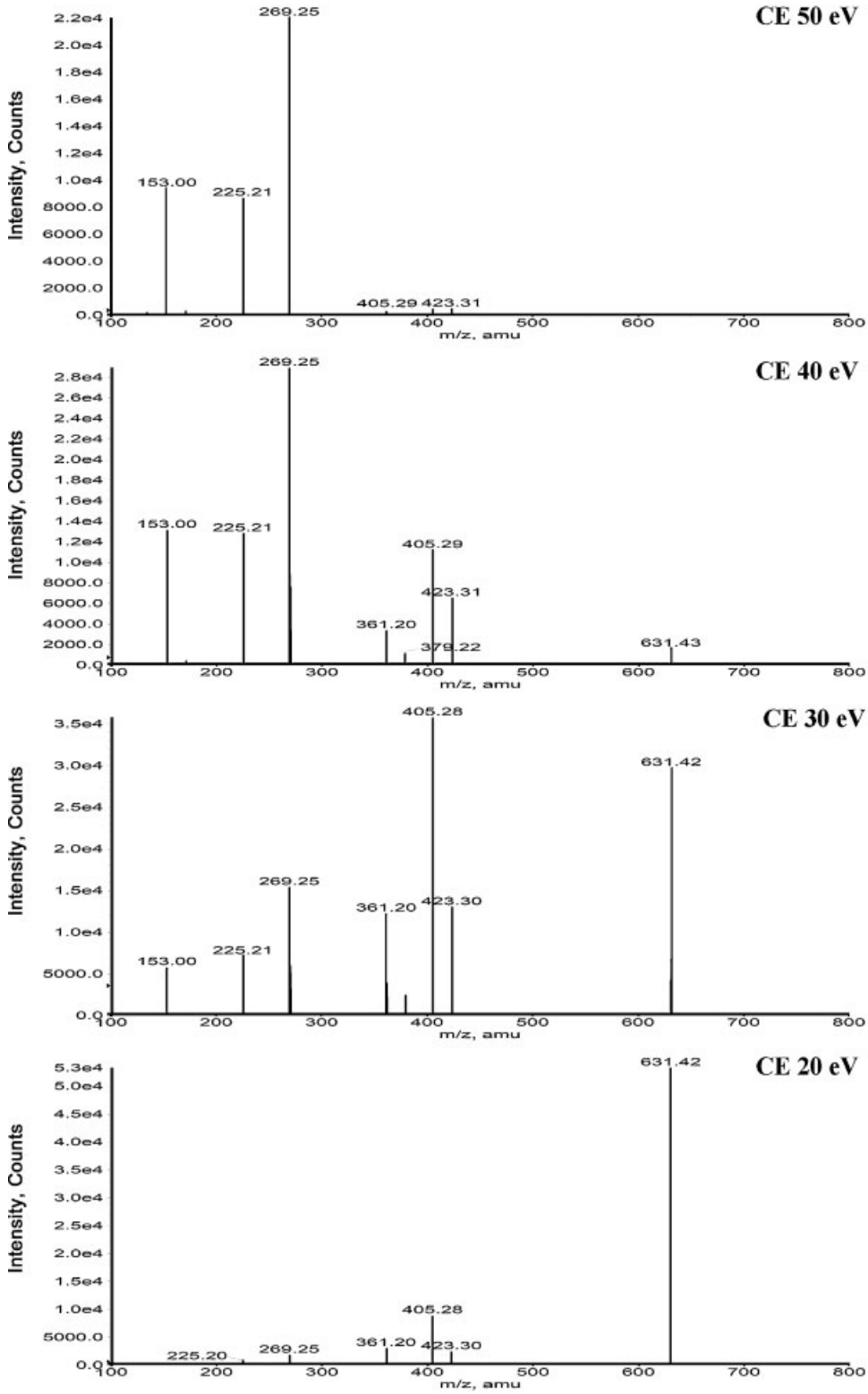

Figure 1. Product ion spectrum of PA(17:0/14:1) recorded on a hybrid quadrupole time-of-flight mass spectrometer (QSTAR Pulsar) at collision energy of 20, 30, 40, and 50 eV, respectively.

Fragmentation patterns of molecular anions of diacyl PS, PG, PI, and PE as a function of collision energy

Fragmentation patterns of PS(17:0/14:1), PG(17:0/14:1), PI(17:0/14:1), and PE(17:0/14:1) at different collision energies were also examined and analyzed following a protocol virtually identical to that used for PA(17:0/14:1). Fragmentation patterns and diagrams showing the structure of these lipids and the bond cleavages of the major fragments of PA(17:0/14:1), PS(17:0/14:1), PG(17:0/14:1), PI(17:0/14:1),

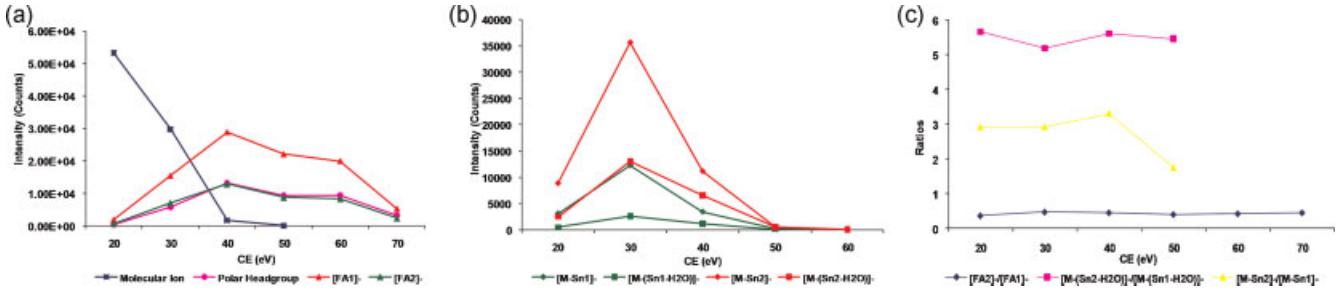

Figure 2. (a) Absolute intensities (ion counts) of molecular ions, polar head group (m/z –153.0), and fatty acyl anions (m/z -225.2 and –269.3) of PA(17:0/14:1) plotted vs. collision energy. (b) Absolute intensities of lyso-form fragment ions $[M–Sn1]^-$, $[M–Sn2]^-$, $[M–(Sn1\text{-}H_2O)]^-$, and $[M–(Sn2\text{-}H_2O)]^-$ of PA(17:0/14:1) plotted vs. collision energy. (c) Ratios of the signal intensities of $[FA2]^-$ vs. $[FA1]^-$, $[M–(Sn2\text{-}H_2O)]^-$ vs. $[M–(Sn1\text{-}H_2O)]^-$, and $[M–Sn2]^-$ vs. $[M–Sn1]^-$ of PA(17:0/14:1).

and PE(17:0/14:1), each recorded at the respective optimum collision energy, are shown in Fig. 3.

It is interesting to note the similarities and differences in the fragmentation patterns among different diacyl glycerophospholipids. PS(17:0/14:1), PG(17:0/14:1), and PI(17:0/14:1) all exhibited sets of lyso-form fragment ions ([M–polar head group–Sn1/2]$^-$ and [M–polar head group–(Sn1/2-H_2O)]$^-$) identical to those for PA(17:0/14:1), corresponding to fragmentation pathways resulting in neutral loss of both fatty acyl moieties and their respective polar head groups.[12,13,15] In contrast, PG(17:0/14:1) and PI(17:0/14:1) each exhibited its own set of lyso-form fragment ions, corresponding to neutral loss of fatty acyl moieties as free fatty acids ([M–Sn1/2]$^-$) or as ketenes ([M–(Sn1/2-H_2O)]$^-$). PS(17:0/14:1) exhibited only the [M–polar head group–Sn1/2]$^-$ and [M–polar head group–(Sn1/2-H_2O)]$^-$ sets of lyso-form fragment ions, identical to the [M–Sn1/2]$^-$ and [M–(Sn1/2-H_2O)]$^-$ fragment ions of PA(17:0/14:1) that of course has no head group. During fragmentation glycerophosphoserines will first shed the serine polar head group and fragment as glycerophosphatidic acids afterwards.[12] Information about m/z values of all the observed lyso-form fragment ions is given in Supplemental Table S1 (see Supporting Information). The lyso-form fragment ions of PE(17:0/14:1) were of relatively low abundance at collision energies around 40 eV, suggesting stronger bonding of the ethanolamine phosphate head group to the glycerol backbone.

Interestingly, it can be seen from Fig. 4(a) that the lyso-form fragment ions [M–Serine-Sn2]$^-$ and [M–Serine–(Sn2-H_2O)]$^-$ of PS(17:0/14:1) are more abundant than [M–Serine-Sn1]$^-$ and [M–Serine-(Sn1-H_2O)]$^-$, respectively. For PG(17:0/14:1) the lyso-form ions [M–Sn2]$^-$, [M–(Sn2-H_2O)]$^-$, and [M–Glycerol-Sn2]$^-$ are more abundant than their respective counterpart ions [M–Sn1]$^-$, [M–(Sn1-H_2O)]$^-$, and [M–Glycerol-Sn1]$^-$. The observed abundances of the lyso-form fragment ions [M–Glycerol-(Sn2-H_2O)]$^-$ and [M–Glycerol-(Sn1-H_2O)]$^-$ were too low to be visualized in the figures (Figs. 4(b) and 4(c)). Similarly for PI(17:0/14:1) the lyso-form ions [M–Sn2]$^-$, [M–(Sn2-H_2O)]$^-$, [M–Inositol–Sn2]$^-$, and [M–Inositol–(Sn2-H_2O)]$^-$ were more abundant than their respective counterpart ions. The signal for the lyso-form fragment ion [M–Inositol–(Sn2-H_2O)]$^-$ was too weak to be visualized in the figures (Figs. 4(d) and 4(e)). Lyso-form fragment ions for PE(17:0/14:1) are of relatively low abundance, but at a collision energy of 40 eV, [M–Sn2]$^-$ and [M–(Sn2-H_2O)]$^-$ ions exhibited higher abundance than [M–Sn1]$^-$ and [M–(Sn1-H_2O)]$^-$ ions (Fig. 4(f)).

These trends were also confirmed in identical experiments performed on PS(12:0/13:0), PS(17:0/20:4), PG(12:0/13:0), PG(17:0/20:4), PI(12:0/13:0), PI(17:0/20:4), PE(12:0/13:0), and PE(17:0/20:4) (Supplemental Figs S2(a)–(h), Supporting Information). It is therefore concluded that the relative abundances of the lyso-form fragment ions of diacyl glycerophospholipids provided reliable structural information to determine the stereospecific information of diacyl glycerophospholipids. For diacyl PA, PS, and PI the lyso-form fragment ions [M–Sn2]$^-$ and [M–polar head group–Sn2]$^-$ are more abundant than their respective [M–(Sn2-H_2O)]$^-$ and [M–polar head group–(Sn2-H_2O)]$^-$ ions, suggesting a more facile process for the neutral loss of free fatty acid than the corresponding neutral loss of ketene; whereas the reverse is observed for diacyl PE (Fig. 4 and Supplemental Fig. S2, see Supporting Information). For diacyl PG the trend is not clear. It was also observed that the optimum collision energy required to record abundant lyso-form fragment ions increases with the length of the fatty acyl chains. The optimum collision energy for PI species is estimated to be above 50 eV whereas it is around 40 eV for other glycerolphospholipids.

It is also worth noting that the relative abundance of the two fatty acyl anions of glycerophosphoinositols depended on collision energy and the characteristics of fatty acyl moieties; whereas the ratios of [M–(Sn2-H_2O)]$^-$/[M–(Sn1-H_2O)]$^-$ and [M–Sn2]$^-$/[M–Sn1]$^-$ are always higher than unity (Supplemental Figs. S3(a)–(c), Supporting Information). Thus for diacyl glycerophosphoinositols the regiospecificity can only be determined through the differential abundance of these lyso-form fragment ions.

Characterization of diacyl glycerophospholipids in lipid extracts from rat hepatoma cells

We next tested the present methodology for the characterization of phospholipids in realistic complex samples. Briefly, lipids were extracted from rat hepatoma cells overexpressing lipin-1α, as described in the Experimental section, and analyzed by our methodology. Lipin-1α functions as phosphatidate phosphatase enzyme in lipid metabolism.[32,33] The identical fatty acyl compositions of glycerophospholipids in different subclasses (with different polar head groups) could possibly link them together into a specific

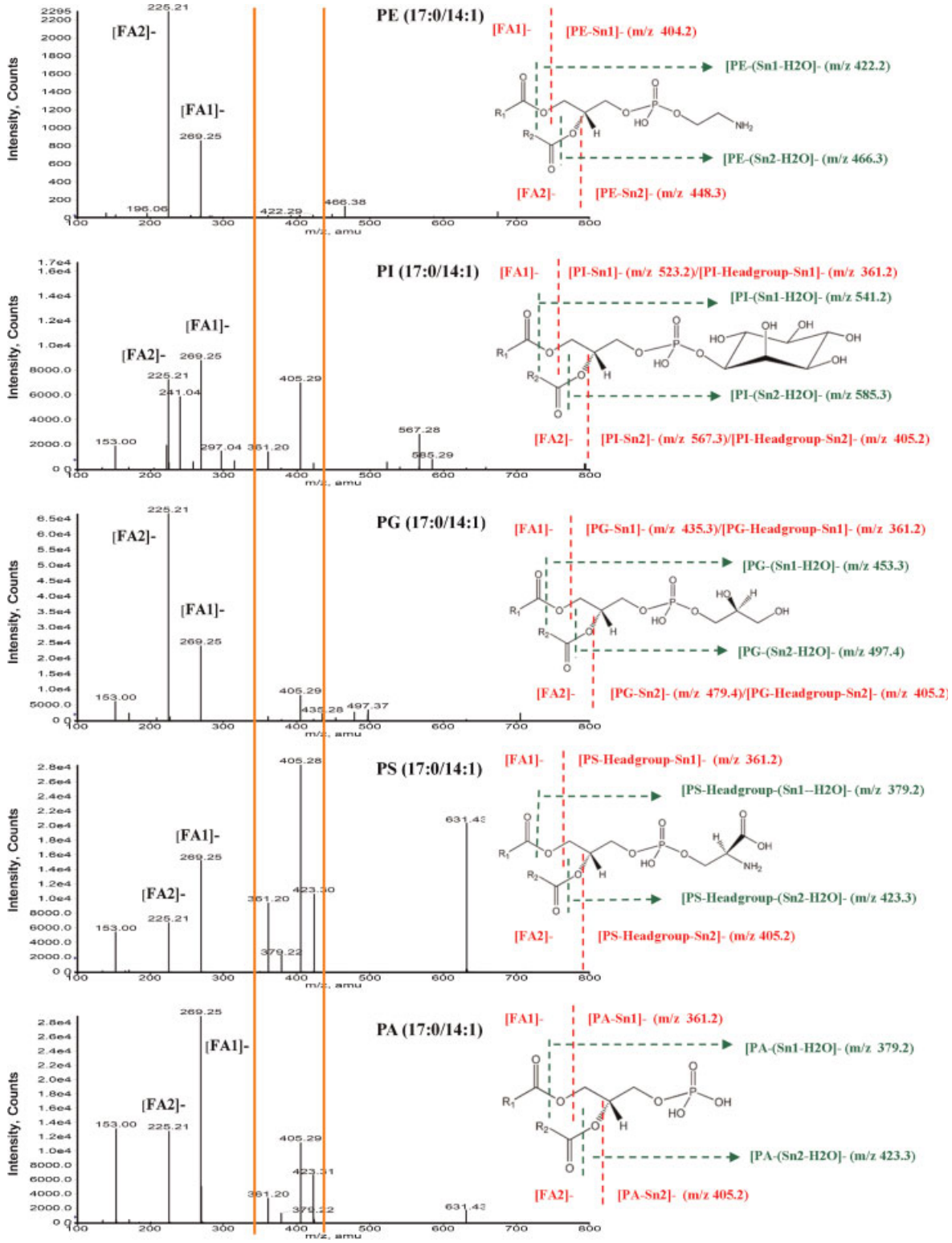

Figure 3. Fragmentation patterns and diagrams showing the structure of these lipids and the bond cleavages of the major fragments of PA(17:0/14:1), PS(17:0/14:1), PG(17:0/14:1), PI(17:0/14:1), and PE(17:0/14:1). The spectrum of PI(17:0/14:1) was recorded at 50 eV; all the other spectra were recorded at 40 eV. The PA, PS, PG, and PI species exhibited identical fragment ions in the region between the two vertical red lines.

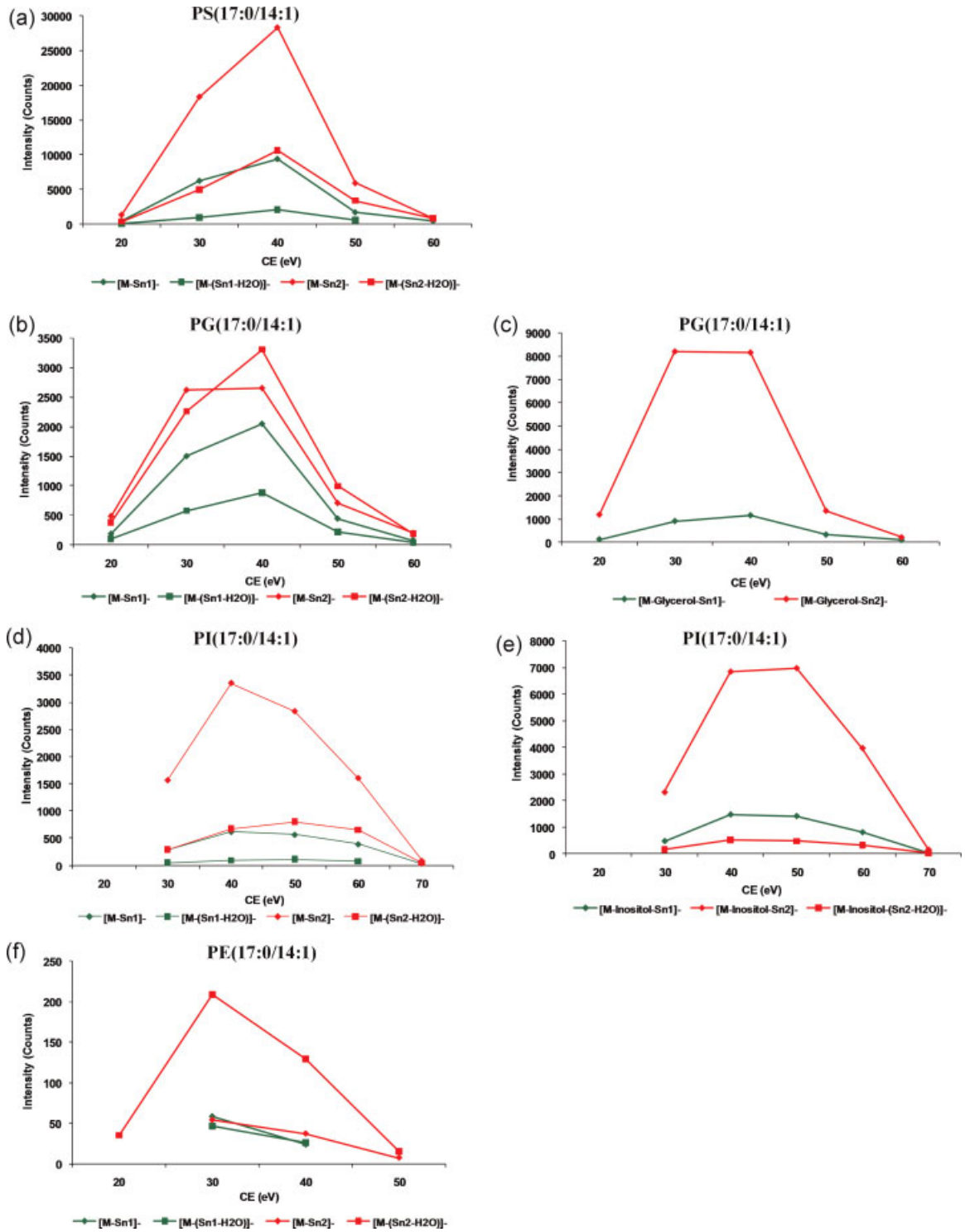

Figure 4. Absolute intensities (ion counts) of lyso-form fragment ions of molecular anions of (17:0/14:1) diacylglycerophospholipids, plotted with respect to collision energy: (a) $[M–Serine–Sn1]^-$, $[M–Serine–Sn2]^-$, $[M–Serine–(Sn1\text{-}H_2O)]^-$, and $[M–Serine–(Sn2\text{-}H_2O)]^-$ of PS; (b) $[M–Sn1]^-$, $[M–Sn2]^-$, $[M–(Sn1\text{-}H_2O)]^-$, and $[M–(Sn2\text{-}H_2O)]^-$ of PG; (c) $[M–Glycerol–Sn1]^-$ and $[M–Glycerol–Sn2]^-$ of PG. Intensities corresponding to $[M–Glycerol–(Sn1\text{-}H_2O)]^-$ and $[M–Glycerol–(Sn2\text{-}H_2O)]^-$ were too low to be measured reliably. (d) $[M–Sn1]^-$, $[M–Sn2]^-$, $[M–(Sn1\text{-}H_2O)]^-$, and $[M–(Sn2\text{-}H_2O)]^-$ of PI (17:0/14:1); (e) $[M–Inositol–Sn1]^-$, $[M–Inositol–Sn2]^-$, and $[M–Inositol–(Sn2\text{-}H_2O)]^-$ of PI. Intensities of $[M–Inositol–(Sn1\text{-}H_2O)]^-$ was too low to be measured reliably. (f) $[M–Sn1]^-$, $[M–Sn2]^-$, $[M–(Sn1\text{-}H_2O)]^-$, and $[M–(Sn2\text{-}H_2O)]^-$ of PE.

metabolic pathway. Testing this hypothesis necessitated a reliable mass spectrometric technique capable of determining the stereospecificity of diacyl glycerophospholipids. In negative ion mode, precursor ion scans for *m/z* –153 and –196 were first performed on the lipid extracts isolated from the lipin-1α overexpressing cell line to highlight PA/PS/PG/PI and PE, respectively (Supplemental Fig. S4, Supporting Information). Molecular anions of diacyl glycerophospholipids were then subjected to fragmentation.

Clearly, in some instances isobaric species will be combined as precursor ions. However, the power of this methodology is that it can differentiate the different isobaric lipid species. For example, Fig. 5 shows the superimposed product ion spectra of the isobaric precursor ions at *m/z* −834.6. The fragment ions at *m/z* −153 ([Glycerophosphate–H_2O]$^-$) and those at *m/z* −747.5 (neutral loss of 87 Da, the serine head group) indicated these lipid species were glycerophosphoserines. The fragment ions at *m/z* −281.3, −283.3, −327.2, and −329.2, corresponding to fatty acyl anions [FA18:1]$^-$, [FA18:0]$^-$, [FA22:6]$^-$, and [FA22:5]$^-$, respectively, suggested the compositions of these lipids to be PS(18:0-22:6) and PS(18:1-22:5) (the stereospecificity is yet to be determined). For diacyl PS the abundance of acyl anions [FA2]$^-$ is lower than that of [FA1]$^-$.[12] The higher intensities of [FA18:1]$^-$ and [FA18:0]$^-$ compared with those of [FA22:5]$^-$ and [FA22:6]$^-$, respectively, allowed the two lipid species to be identified as PS(18:0/22:6) and PS(18:1/22:5) (the stereospecificity is determined), respectively. Abundant fragment ions are also observed at *m/z* −419.3, −437.3, −463.3, and −481.3, corresponding to [M–Serine–FA22:6]$^-$, [M–Serine–(FA22:6-H_2O)]$^-$, [M–Serine–FA18:0]$^-$, and [M–Serine–(FA18:0-H_2O)]$^-$, respectively. The ions corresponding to [M–Serine–FA22:6]$^-$ (*m/z* −419.3) and [M–Serine–(FA22:6-H_2O)]$^-$ (*m/z* −437.3) exhibited higher abundances than [M–Serine–FA18:0]$^-$ (*m/z* -463.3) and [M–Serine–(FA18:0-H_2O)]$^-$ (*m/z* −481.3), respectively, thus allowing definitive identification of PS(18:0/22:6). Similarly, PS(18:1/22:5) can be identified on the basis that the lyso-form fragment ions at *m/z* −417.3 and −435.3 were observed at higher abundances than their respective counterpart ions. In this case the structural

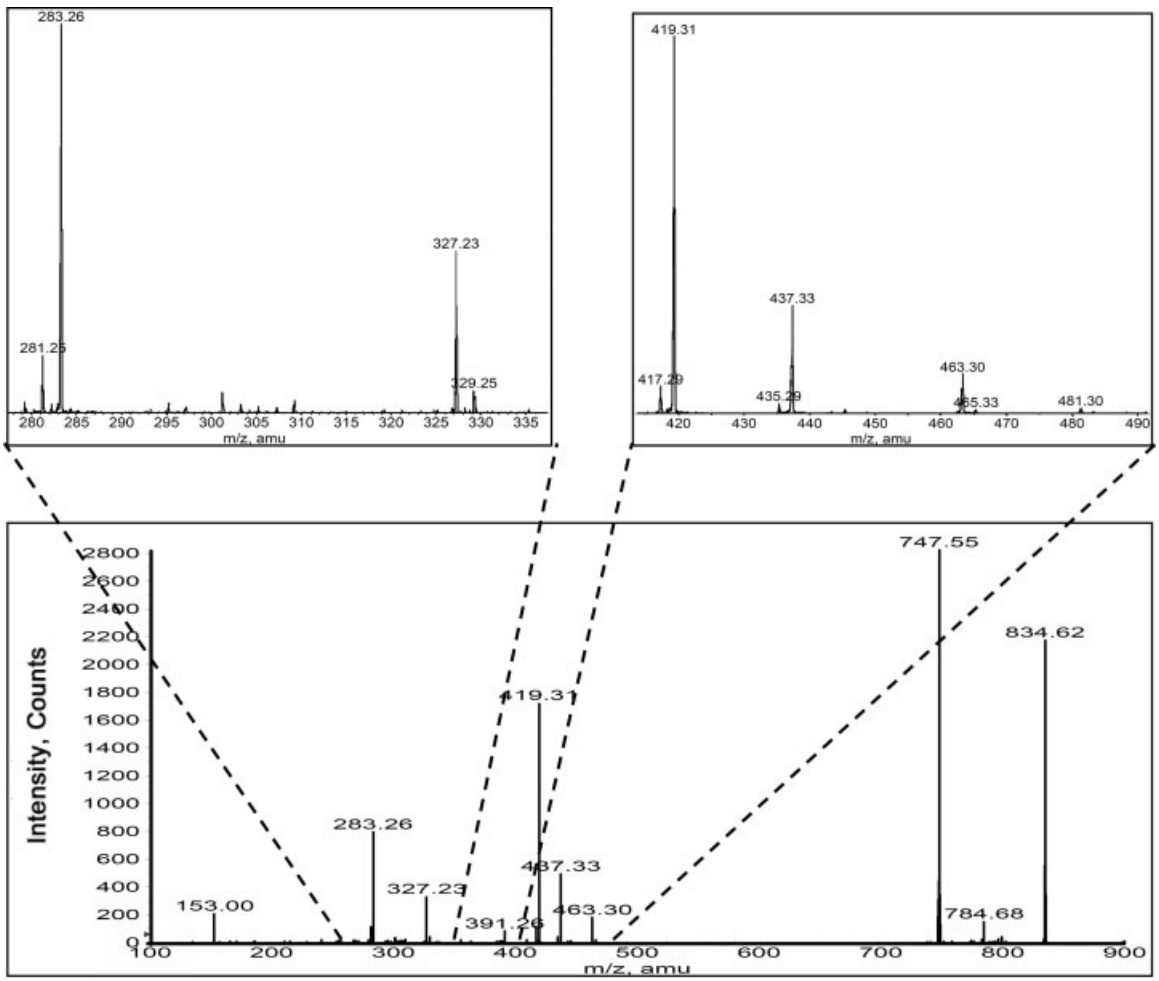

Figure 5. The overlapped product ion spectrum of molecular anions of the isobaric lipid species PS(18:0/22:6) and PS(18:1/22:5) at *m/z* −834.6. Fragment ions at *m/z* −153 correspond to [Glycerophosphate–H_2O]$^-$ and those at *m/z* −747.5 to neural loss of 87 Da (the serine head group). Fragment ions at *m/z* −281.3, −283.3, −327.2, and −329.2, corresponding to fatty acyl anions [FA18:1]$^-$, [FA18:0]$^-$, [FA22:6]$^-$, and [FA22:5]$^-$, respectively. For PS(18:0/22:6), lyso-form fragment ions are observed at *m/z* −419.3, −437.3, −463.3, and −481.3, corresponding to [M–Serine–FA22:6]$^-$, [M–Serine–(FA22:6-H_2O)]$^-$, [M–Serine–FA18:0]$^-$, and [M–Serine–(FA18:0-H_2O)]$^-$, respectively. Fragment ions at *m/z* −417.3 and −435.3 are lyso-form fragment ions from PS(18:1/22:5).

information based on either the fatty acyl anions or the lyso-form fragment ions allowed the lipid species of interest to be exclusively determined.

Figure 6 shows a second example of a mixed product ion spectrum of molecular anions of isobaric lipid species at *m/z* −885.5. The fragment ions at *m/z* −153 ([Glycerophosphate–H_2O]$^-$), −223 ([Inositolphosphate–$2H_2O$]$^-$), −241 ([Inositolphosphate–H_2O]$^-$), and −259 ([Inositolphosphate]$^-$) indicated that these lipid species were glycerophosphoinositols. The fragment ions at *m/z* −281.3, −283.3,

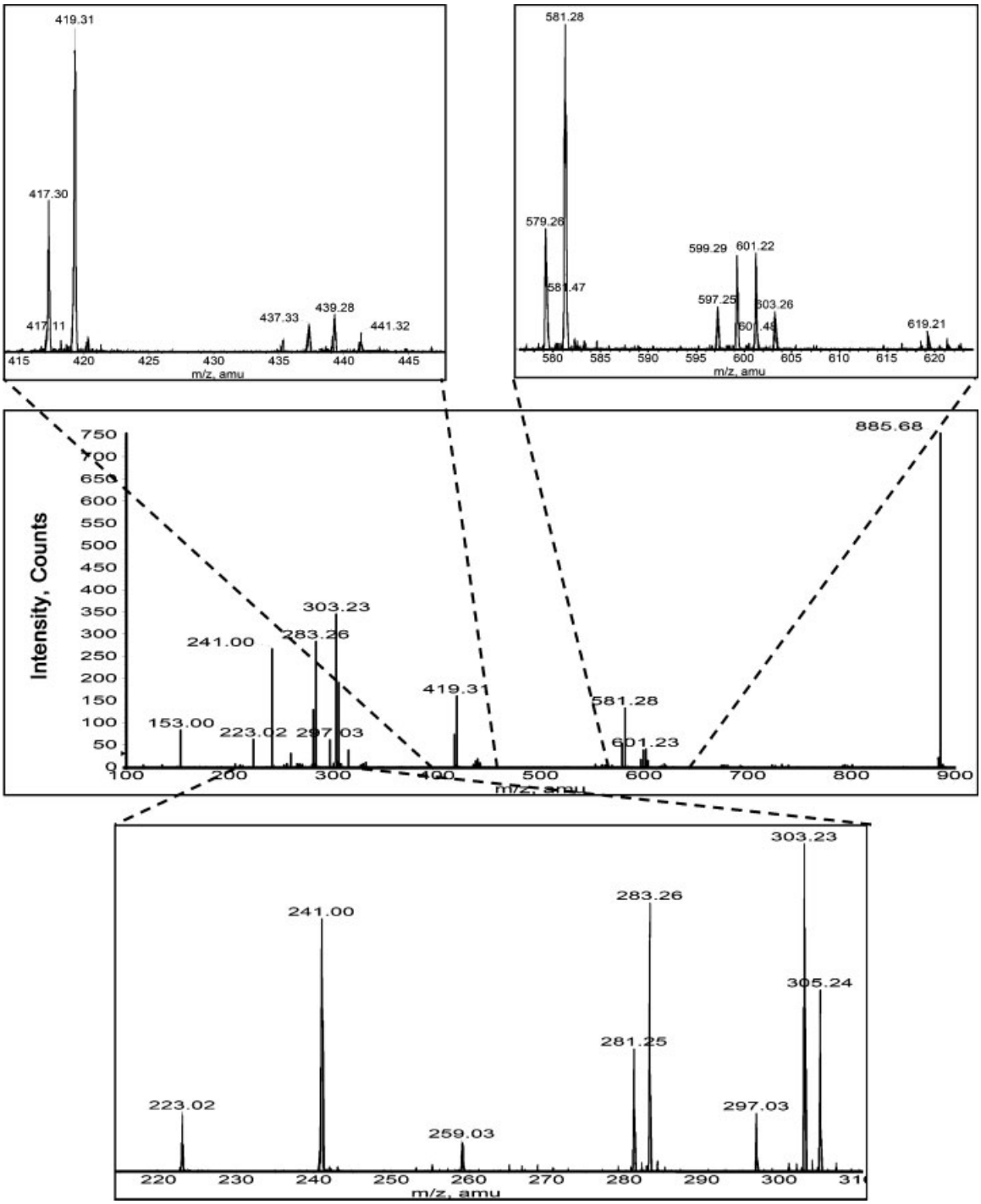

Figure 6. The overlapped product ion spectrum of molecular anions of the isobaric lipid species PI(18:0/20:4) and PI(18:1/20:3) at *m/z* –885.5. Fragment ions at *m/z* −153, −223, −241, and −259 correspond to [Glycerophosphate–H_2O]$^-$, [Inositolphosphate–$2H_2O$]$^-$, [Inositolphosphate–H_2O]$^-$, and [Inositolphosphate]$^-$, respectively. Fragment ions at *m/z* −281.3, −283.3, −303.2, and −305.2, correspond to fatty acyl anions [FA18:1]$^-$, [FA18:0]$^-$, [FA20:4]$^-$, and [FA20:3]$^-$, respectively. For PI(18:0/20:4), the lyso-form fragment ions are observed at *m/z* −601.3, −619.3, −581.3, and −599.3, corresponding to [M–FA18:0]$^-$, [M–(FA18:0-H_2O)]$^-$, [M–FA20:4]$^-$, and [M–(FA20:4-H_2O)]$^-$, respectively. For PI(18:1/20:3), lyso-form fragment ions are at *m/z* −579.3, −597.3, −603.3, and −621.3. Peaks at *m/z* −417.3 and −419.3 correspond to lyso-form fragment ions [M–Inositol–FA20:3]$^-$ and [M–Inositol–FA20:4]$^-$, respectively.

−303.2, and −305.2, corresponding to fatty acyl anions $[FA18:1]^-$, $[FA18:0]^-$, $[FA20:4]^-$, and $[FA20:3]^-$, respectively, suggested the compositions of these lipids were PI(18:0-20:4) and PI(18:1-20:3), respectively. The relative abundance of the two fatty acyl anions of diacyl glycerophosphoinositols depends on the collision energy and the length of the fatty acyl moieties, therefore the stereospecific positions of the two fatty acyl chain have to be determined via the relative abundances of their lyso-form fragments.[15] For PI(18:0-20:4), the lyso-form fragment ions can be found at *m/z* 601.3, 619.3, 581.3, and 599.3, corresponding to $[M–FA18:0]^-$, $[M–(FA18:0\text{-}H_2O)]^-$, $[M–FA20:4]^-$, and $[M–(FA20:4\text{-}H_2O)]^-$, respectively. The intensities of peak at *m/z* −581.3 ($[M–FA20:4]^-$) and −599.3 ($[M–(FA20:4\text{-}H_2O)]^-$) are higher than those at *m/z* −601.3 ($[M–FA18:0]^-$) and −619.3 ($[M–(FA18:0\text{-}H_2O)]^-$), respectively, thus allowing the assignment of FA20:4 to *sn*2 and FA18:0 to *sn*1. It followed that the complete structure of the lipid species of interest was PI(18:0/20:4). Similarly, PI(18:1/20:3) was determined on the basis that the lyso-form fragment ions at *m/z* −579.3 and −597.3 exhibited higher intensities than those at *m/z* −603.3 and −621.3, respectively. The assignment of the stereospecific structure of PI(18:0/20:4) and PI(18:1/20:3) can also be achieved on the basis of higher peak intensities at *m/z* −417.3 ($[M–Inositol–FA20:3]^-$) and −419.3 ($[M–Inositol–FA20:4]^-$) than those of their respective counterpart ions. To the best of our knowledge this is the first time that the stereospecificities of diacyl glycerophosphoinositols from lipid extracts of biological samples have been determined based on their tandem mass spectra.

Shotgun lipidomic approaches usually analyze lipid extracts without or with very little pre-purification.[1,28,29] Most lipid species are identified under conditions subject to interferences from other isobaric species (or lipid species with molecular ion mass included within the isolation window for precursor ions) of the same class or other classes. As a result, the peak intensities of some fatty acyl anions recorded in a tandem mass spectrum often include contributions from different lipid species. Figure 7 demonstrates that even isobaric lipids from different subclasses can be successfully identified using the present methodology. The product ion spectrum for the precursor at *m/z* −762.5 shows fragment ions at *m/z* −153 ($[Glycerophosphate–H_2O]^-$), −196 ($[Ethanolaminephosphate–H_2O]^-$), and −675.5 (neutral loss of 87 Da, the serine head group), indicating that the precursor at a nominal *m/z* value of -762.5 is a mixture of several isobaric PE and PS lipid species. Following the methodology discussed above, PE(18:1/20:5), PE(18:2/20:4), PE(16:0/22:6), and PE(16:1/22:5) can be identified on the basis of structural information associated with both the fatty acyl anions and the lyso-form fragment ions (for diacyl PE species the fragment anion $[FA2]^-$ exhibited higher abundance than $[FA1]^-$).[14] In addition PS(16:0-18:0) can also be confirmed to be present in the mixture. Unfortunately, its stereospecific information could not be determined on the basis of the relative abundance of their two fatty acyl anions $[FA16:0]^-$ (*m/z* −255.2) and $[FA18:0]^-$ (*m/z* −283.2), which were virtually equal. However, the stereospecificity can be established based on the lyso-form fragment ion $[M–Serine–FA16:0]^-$ (*m/z* −419.3), which exhibited higher intensity than $[M–Serine–FA18:0]^-$ (*m/z* −391.3), and confirmed the presence of PS(18:0/16:0). The fragmentation of PS(18:0/16:0) by itself would result in a noticeable lower intensity of $[FA16:0]^-$ (*m/z* -255.2) than that of $[FA18:0]^-$ (*m/z* −283.2), as the fatty acyl anion $[FA2]^-$ of a diacyl PS should exhibit lower abundance than $[FA1]^-$.[12] However, in this case the intensity of $[FA16:0]^-$ (*m/z* −255.2) also contained partial contributions from PE(16:0/22:6). The overlapping of $[FA16:0]^-$ from two different lipid species compromised the abundance ratio between $[FA16:0]^-$ (*m/z* −255.2) and $[FA18:0]^-$ (*m/z* −283.2) and thus prevented the determination of fatty acyl chain positions of PS(18:0/16:0) on the basis of this abundance ratio. The lyso-form fragment ions allowed the stereospecific information to be unambiguously determined. Also there is no overlap between the lyso-form fragment ions of PE and PS. The lyso-form fragment ions of PE have even nominal *m/z* values while those of PS have odd nominal values.

Table 1 lists the identified diacyl glycerophospholipids from the cell extracts of lipin-1α-overexpressing cells, including PS, PE, PI, PA, and PG species. This result demonstrates that the novel methodology reported in this work can be employed to determine the stereospecificity of all glycerophospholipids that are preferentially ionized in negative ion mode. The stereospecificity of the vast majority of the lipid species can be consistently elucidated based on the structural information obtained from either the fatty acyl anions or the lyso-form ions (in black). Around 30% of the listed diacyl glycerophospholipids were identified primarily based on the lyso-form ions (in red boldface). These lipids included the diacyl glycerophosphoinositols, for which the stereospecificity cannot be identified on the basis of their fatty acyl anions (∼10%), and other diacyl glycerophospholipids, for which the relative abundances of the fatty acyl anions of interest were either too close to call or lead to opposite positional isomers (∼20%). As mentioned previously these fatty acyl anions were most likely overlapped with those from other lipid species. The determination of the fatty acyl positions for diacyl PE species represented the most challenging task, owing to the relatively lower abundance of the lyso-form ions and possible interferences from PC species. As a result, the fatty acyl chain positions of several diacyl PE species were proposed only based on the relative abundance of their acyl anions (in blue italic).

The ultimate solution for comprehensive determination of the stereospecific information of diacyl glycerophospholipids would likely necessitate the integration of front-end chromatographic separation. Nevertheless, diacyl PE species were identified in this work primarily based on the structural information from the lyso-form fragment ions without any chromatographic separation. Furthermore, the lipid species primarily identified on the basis of lyso-form fragment ions, such as PA(18:0/20:3), PG(18:0/16:1), PI(18:0/18:2), PI(16:0/20:2), PI(18:0/20:4), PI(18:0/20:3), PE(16:0/20:2), PE(16:0/22:4), and PE(16:0/22:3), have stereospecificities in agreement with the biochemistry convention, that assigns the saturated fatty acyl to the *sn*1 position and the poly-unsaturated fatty acyl to the *sn*2 position. It is interesting to note that stereospecificity of PE(18:1/16:1), which was determined primarily based on the lyso-form fragment ions, was consistent with PS(18:1/16:1), which was identified based on the structural information of both acyl anions and lyso-form ions. Similarly PE(18:1/20:2) and PI(18:1/20:2) were consistent with PA(18:1/20:2), where the former two were identified primarily based on the lyso-form fragment ions and the latter was identified based on the structural information of both acyl anions and lyso-form ions. It is also interesting to note that the stereospecificities of some

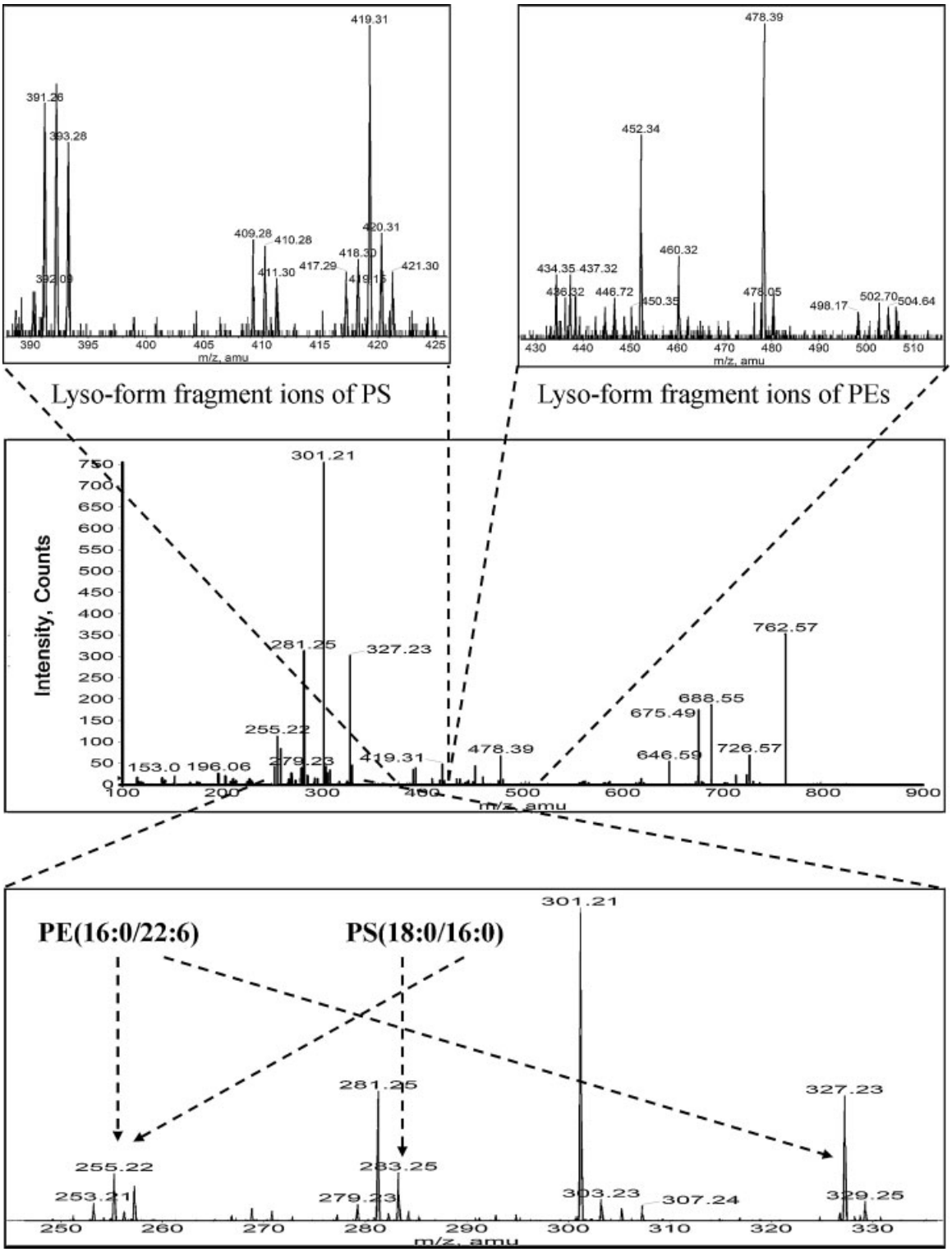

Figure 7. The overlapped product ion spectrum of molecular anions of the isobaric lipid species PE(18:1/20:5), PE(18:2/20:4), PE(16:0/22:6), PE(16:1/22:5), and PS(18:0/16:0) at m/z –762.5. Fragment ions at m/z −153 ([Glycerophosphate–H_2O]$^-$), −196 ([Ethanolaminephosphate–H_2O]$^-$), and −675.5 (neutral loss of 87 Da, the serine head group) indicate the presence of a mixture of several isobaric PE and PS lipid species. Lyso-form fragment ions of PE(18:1/20:5), PE(18:2/20:4), PE(16:0/22:6), and PE(16:1/22:5) are observed at even nominal m/z values while lyso-form fragment ions of PS(18:0/16:0) are at odd nominal m/z. The intensity of [FA16:0]$^-$ (m/z 255.2) contained contributions from both PE(16:0/22:6) and PS(18:0/16:0).

Table 1. List of diacyl glycerophospholipids identified and their relative abundance with respect to the base peak. Lipid species in normal typeface are those for which the stereospecificity is consistently elucidated based on the structural information obtained from either the fatty acyl anions or the lyso-form ions. Lipid species in bold are those for which the stereospecificity is identified primarily based on the lyso-form ions, including the diacyl glycerophosphoinositols, for which the stereospecificity cannot be identified on the basis of their fatty acyl anions, and other diacyl glycerophospholipids, for which the relative abundances of the fatty acyl anions of interest were either too close to call or lead to opposite positional isomers. Lipid species in italic are those for which the stereospecificity is proposed only based on the relative abundance of their acyl anions

Lipid class	*m/z*	% of base peak	Lipid species
PA	725.4	37.6	PA(18:1/20:2)
			PA(18:2/20:1)
			PA(18:0/20:3)
PG	747.9	16.8	PG(16:0/18:1)
			PG(18:0/16:1)
PI	861.6	28.8	**PI(18:0/18:2)**
			PI(18:1/18:1)
			PI(16:0/20:2)
	885.6	38.4	**PI(18:0/20:4)**
			PI(18:1/20:3)
	887.7	36	**PI(18:0/20:3)**
			PI(18:1/20:2)
PS	732.3	16	PS(16:0/16:1)
	758.4	23.2	PS(16:0/18:2)
			PS(18:1/16:1)
	760.5	46.4	PS(16:0/18:1)
			PS(18:0/16:1)
	762.5	17.6	**PS(18:0/16:0)**
	782.4	20.8	PS(16:0/20:4)
			PS(18:1/18:3)
			PS(18:2/18:2)
	784.5	26.4	PS(16:0/20:3)
			PS(18:0/18:3)
			PS(18:1/18:2)
	786.6	64	PS(18:0/18:2)
			PS(18:1/18:1)
			PS(16:0/20:2)
	788.4	42.4	PS(18:0/18:1)
	808.5	36.8	PS(18:0/20:5)
			PS(18:1/20:4)
	810.6	48.8	PS(18:0/20:4)
			PS(18:1/20:3)
	812.4	52.8	PS(18:0/20:3)
	834.6	100	PS(18:0/22:6)
			PS(18:1/22:5)
	836.4	62.4	PS(18:0/22:5)
	862.5	32	PS(20:0/22:6)
			PS(20:1/22:5)
PE	714.5	58.2	PE(16:0/18:2)
			PE(18:1/16:1)
	716.6	94.5	PE(16:0/18:1)
			PE(18:0/16:1)
	736.4	52.7	PE(16:0/20:5)
			PE(16:1/20:4)
	738.5	65.5	PE(16:0/20:4)
			PE(16:1/20:3)
			PE(18:2/18:2)
			PE(18:1/18:3)
	740.3	72.7	PE(16:0/20:3)
			PE(20:2/16:1)
			PE(18:0/18:3)
			PE(18:1/18:2)
	742.7	85.5	**PE(16:0/20:2)**
			PE(18:1/18:1)
			PE(18:0/18:2)
	744.8	43.6	*PE(16:0/20:1)*
			PE(18:0/18:1)
	762.2	60	PE(16:0/22:6)
			PE(18:1/20:5)
			PE(18:2/20:4)
	764.6	100	PE(18:0/20:5)
			PE(18:1/20:4)
	766.7	96.4	PE(18:0/20:4)
			PE(18:1/20:3)
			PE(16:0/22:4)
	768.5	40	**PE(16:0/22:3)**
			PE(18:0/20:3)
			PE(20:1/18:2)
			PE(18:1/20:2)
	788.3	18.2	**PE(18:1/22:6)**
	790.1	30.9	PE(18:0/22:6)
			PE(18:1/22:5)

(*Continues*)

diacyl glycerophospholipids, identified primarily based on the lyso-form fragment ions, were consistent across different subclasses taking PS(18:1/18:3) and PE(18:1/18:3), and PS(18:1/20:3), PE(18:1/20:3), and PI(18:1/20:3) as examples. These results suggested that lyso-form fragment ions provided reliable structural information for the determination of stereospecificity of diacyl glycerophospholipids. Conveniently, this structural information was readily available from MS^2 mass spectra recorded on a hybrid quadrupole time-of-flight mass spectrometer.

MPIS, FAS, and MDMS-SL mass spectrometric techniques have proved to be powerful shotgun lipidomic approaches for comprehensive lipid profiling of complex lipid extracts from various biological systems.[1,28,29] However, the vast majority of lipid species are analyzed under conditions such that interferences from other isobaric species (or lipid species with molecular ion mass covered by the mass window for precursor ion selection) arise from the same or other lipid classes. As a result, the abundance of the fatty acyl anions of interest very likely contained contributions from more than one lipid species. It follows that it is very difficult to accurately determine the stereospecific information for diacyl glycerophospholipids when only the relative abundance of the two fatty acyl anions is considered. Furthermore, lipid species that are not in fact present could be wrongfully inferred to be present by combining two fatty acyl anions which are in fact from different lipid species. The lyso-form fragment ions provided reliable structural information for accurate determination of the stereospecific information of diacyl glycerophospholipids, including diacyl glycerophosphoinositols.

CONCLUSIONS

In this work, we developed a novel approach for the determination of fatty acyl positions of diacyl glycerophospholipids, including PA, PS, PG, PI, and PE, for which all the structural information was obtained from MS^2 mass spectra recorded using a hybrid quadrupole time-of-flight mass spectrometer. We first fully examined the fragmentation patterns of a variety of diacyl glycerophospholipid standards over a wide range of collision energy. For all the diacyl glycerophospholipid standards examined it was found that the lyso-form fragment ions corresponding to the neutral loss of fatty acids from the *sn*2 position consistently exhibited higher abundance than those corresponding to the neutral loss from *sn*1 position on the glycerol backbone. We then demonstrated the feasibility of determining the stereospecific information for diacyl glycerophospholipids in a lipid extract from rat hepatoma cell line, primarily on the basis of lyso-form fragment ions. We demonstrated that this new methodology is capable of accurately determining the stereospecific information for diacyl glycerophospholipids even with the interferences from isobaric lipid species and without chromatographic pre-separation. In addition, the approach is capable of locating the fatty acyl moieties of diacyl glycerophosphoinositols, which is impossible for methodologies that examine only structural information provided by the fatty acyl anions. Combining the novel methodology reported in this work with the currently widely practiced mass spectrometric techniques such as MPIS, FAS, and MDMS-SL should enable a reliable and convenient platform for comprehensive glycerophospholipid profiling.

SUPPORTING INFORMATION

Additional supporting information may be found in the online version of this article.

Acknowledgements

Daniel Figeys is a Canada Research Chair in Proteomics and Systems Biology, a Professor in the Department of Biochemistry, Microbiology, and Immunology, and Director of the Ottawa Institute of Systems Biology at the University of Ottawa. This work was partially funded through the Canada Research Chair, CIHR grant, and La Fondation Lévesque. Steffany Bennett is the Director of the CIHR Training Program in Neurodegenerative Lipidomics and an Associate Professor in the Department of Biochemistry, Microbiology, and Immunology, and Director of the Ottawa Institute of Systems Biology at the University of Ottawa. This work was partially funded through the Canada Research Chair and La Fondation Lévesque to DF and a CIHR operating (MOP89999) and training grants (TGF 96921) to DF and SALB. Weimin Hou is grateful for financial support from NSERC, OGS, the Institute of Aging and CIHR Training Program in Neurodegenerative Lipidomics, and University of Ottawa. The authors would like to thank Dr. R. K. Boyd, Alexandre P. Blanchard and Sarah Gelbard for their constructive comments and edits.

REFERENCES

[1] X. Han, R. W. Gross. *Mass Spectrom. Rev.* **2005**, *24*, 367.
[2] M. R. Wenk. *Nat. Rev. Drug Discov.* **2005**, *4*, 594.
[3] M. R. Wenk, L. Lucast, G. Di Paolo, A. J. Romanelli, S. F. Suchy, R. L. Nussbaum, G. W. Cline, G. I. Shulman, W. McMurray, P. De Camilli. *Nat. Biotechnol.* **2003**, *21*, 813.
[4] M. Pulfer, R. C. Murphy. *Mass Spectrom. Rev.* **2003**, *22*, 332.
[5] W. Hou, H. Zhou, F. Elisma, S. A. Bennett, D. Figeys. *Brief Funct. Genomic Proteomics* **2008**, *7*, 395.
[6] S. Milne, P. Ivanova, J. Forrester, H. Alex Brown. *Methods* **2006**, *39*, 92.
[7] C. S. Ejsing, J. L. Sampaio, V. Surendranath, E. Duchoslav, K. Ekroos, R. W. Klemm, K. Simons, A. Shevchenko. *Proc. Natl. Acad. Sci. USA* **2009**, *106*, 2136.
[8] R. Aebersold, M. Mann. *Nature.* **2003**, *422*, 198.
[9] L. Yetukuri, K. Ekroos, A. Vidal-Puig, M. Oresic. *Mol. Biosyst.* **2008**, *4*, 121.
[10] M. Oresic, V. A. Hanninen, A. Vidal-Puig. *Trends Biotechnol.* **2008**, *26*, 647.
[11] F. F. Hsu, J. Turk. *J. Am. Soc. Mass Spectrom.* **2000**, *11*, 797.
[12] F. F. Hsu, J. Turk. *J. Am. Soc. Mass Spectrom.* **2005**, *16*, 1510.
[13] F. F. Hsu, J. Turk. *J. Am. Soc. Mass Spectrom.* **2001**, *12*, 1036.
[14] F. F. Hsu, J. Turk. *J. Am. Soc. Mass Spectrom.* **2000**, *11*, 892.
[15] F. F. Hsu, J. Turk. *J. Am. Soc. Mass Spectrom.* **2000**, *11*, 986.
[16] F. F. Hsu, J. Turk. *J. Mass Spectrom.* **2000**, *35*, 595.
[17] X. Han, R. W. Gross. *J. Am. Soc. Mass Spectrom.* **1995**, *6*, 1202.
[18] F. F. Hsu, A. Bohrer, J. Turk. *J. Am. Soc. Mass Spectrom.* **1998**, *9*, 516.
[19] Y. P. Ho, P. C. Huang, K. H. Deng. *Rapid Commun. Mass Spectrom.* **2003**, *17*, 114.
[20] F. F. Hsu, J. Turk. *J. Am. Soc. Mass Spectrom.* **2003**, *14*, 352.
[21] T. Houjou, K. Yamatani, M. Imagawa, T. Shimizu, R. Taguchi. *Rapid Commun. Mass Spectrom.* **2005**, *19*, 654.
[22] E. Vernooij, J. Brouwers, J. Kettenes-van den Bosch, D. Crommelin. *J. Sep. Sci.* **2002**, *25*, 285.
[23] E. Hvattum, G. Hagelin, A. Larsen. *Rapid Commun. Mass Spectrom.* **1998**, *12*, 1405.
[24] K. Yang, H. Cheng, R. W. Gross, X. Han. *Anal. Chem.* **2009**, *81*, 4356.
[25] C. S. Ejsing, E. Duchoslav, J. Sampaio, K. Simons, R. Bonner, C. Thiele, K. Ekroos, A. Shevchenko. *Anal. Chem.* **2006**, *78*, 6202.
[26] K. Ekroos, I. V. Chernushevich, K. Simons, A. Shevchenko. *Anal. Chem.* **2002**, *74*, 941.
[27] D. Schwudke, J. Oegema, L. Burton, E. Entchev, J. T. Hannich, C. S. Ejsing, T. Kurzchalia, A. Shevchenko. *Anal. Chem.* **2006**, *78*, 585.
[28] X. Han, J. Yang, H. Cheng, H. Ye, R. W. Gross. *Anal. Biochem.* **2004**, *330*, 317.
[29] X. Han, R. W. Gross. *J. Lipid Res.* **2003**, *44*, 1071.
[30] K. Ekroos, C. S. Ejsing, U. Bahr, M. Karas, K. Simons, A. Shevchenko. *J. Lipid Res.* **2003**, *44*, 2181.
[31] A. Larsen, S. Uran, P. B. Jacobsen, T. Skotland. *Rapid Commun. Mass Spectrom.* **2001**, *15*, 2393.
[32] K. Reue, D. N. Brindley. *J. Lipid Res.* **2008**, *49*, 2493.
[33] M. Bou Khalil, M. Sundaram, H. Y. Zhang, P. H. Links, J. F. Raven, B. Manmontri, M. Sariahmetoglu, K. Tran, K. Reue, D. N. Brindley, Z. Yao. *J. Lipid Res.* **2009**, *50*, 47.
[34] M. Peterfy, J. Phan, K. Reue. *J. Biol. Chem.* **2005**, *280*, 32883.
[35] C. Chen, H. Okayama. *Mol. Cell. Biol.* **1987**, *7*, 2745.
[36] K. Tran, G. Thorne-Tjomsland, C. J. DeLong, Z. Cui, J. Shan, L. Burton, J. C. Jamieson, Z. Yao. *J. Biol. Chem.* **2002**, *277*, 31187.

